Veterinary Microbiology 314 (2026) 110908

Contents lists available at ScienceDirect

Veterinary Microbiology

journal homepage: www.elsevier.com/locate/vetmic

# Whole-genome analysis of *Ornithobacterium rhinotracheale* from turkeys in Poland: Insights into global diversity, virulence, and antimicrobial resistance

Marek Blanda [a], Olimpia Kursa [b,1], Joanna Kowalczyk [c], Marcin Śmiałek [c,d,*,1]

[a] *Nativet Veterinary Clinic, ul. Piotrowskiego 10e, Olsztyn 10-692, Poland*
[b] *Department of Bacteriology and Bacterial Animal Diseases, National Veterinary Research Institute, al. Partyzantów 57, Puławy 24-100, Poland*
[c] *Department of Poultry Diseases, Faculty of Veterinary Medicine, University of Warmia and Mazury, ul. Oczapowskiego 14, Olsztyn 10-719, Poland*
[d] *Veterinary Diagnostic Laboratory SLW BIOLAB, ul. Grunwaldzka 62, Ostróda 14-100, Poland*

ARTICLE INFO

*Keywords:*
*Ornithobacterium rhinotracheale*
Whole-genome sequencing
MLST
SNP
Antimicrobial resistance

ABSTRACT

*Ornithobacterium rhinotracheale* (ORT) is an emerging avian respiratory pathogen of global concern, causing significant economic losses, particularly in turkeys. Although its distribution is worldwide, genomic data from different geographic regions remain scarce, limiting understanding of its genetic diversity, virulence-associated features, and antimicrobial resistance profiles. In this study, we performed whole-genome sequencing of 49 *O. rhinotracheale* isolates recovered from respiratory tract and joint lesions during outbreaks of ornithobacteriosis in turkeys in Poland to characterize sequence types and explore the genomic diversity and the distribution of virulence- and resistance-associated genes. Comparative multilocus sequence typing revealed high genetic heterogeneity, including three novel sequence types (ST46, ST50, ST51), highlighting ongoing local diversification within a globally distributed pathogen. Whole-genome core single nucleotide polymorphism (SNP)–based phylogenetic analysis further resolved genetic relationships among isolates and identified major genomic clusters. Genomic profiling identified several virulence-associated genes and insertion sequences, including IS4351 and ISMlu9. Distinct resistance gene patterns observed between major STs (ST3, ST46) were observed. These findings provide new insights into the genomic diversity of *O. rhinotracheale* populations and contribute to a broader understanding of its epidemiology and antimicrobial resistance in poultry worldwide.

## 1. Introduction

Ornithobacteriosis is recognized as a disease of high importance in turkey and chicken production, as it compromises animal welfare and causes substantial economic losses worldwide. The etiological agent, *Ornithobacterium rhinotracheale* (ORT), is a Gram-negative, pleomorphic, rod-shaped bacterium belonging to the family Flavobacteriaceae within the phylum Bacteroidota (Abd El-Ghany, 2021). ORT is primarily associated with respiratory disease in turkeys and chickens, including pneumonia and airsacculitis, and has been implicated in pathological conditions such as tracheitis, sinusitis, pericarditis, and pneumonia since its first description in the 1990s. Infection may result in reduced weight gain, impaired feed conversion, increased mortality, and, in breeder flocks, decreased egg production and hatchability (Abd El-Ghany, 2021; Vandamme et al., 1994). Although ORT primarily causes respiratory disease, it can also affect the musculoskeletal system of turkeys, causing arthritis, tenosynovitis, and other joint pathologies (Abd El-Ghany, 2021; Vandamme et al., 1994). The pathogen has been detected not only in turkeys and chickens but also in a broad spectrum of domestic and wild bird species, including ducks, geese, pigeons, and falcons, underscoring its ecological versatility and potential for cross-species transmission (Vandamme et al., 1994; Devriese et al., 1995).

Traditional diagnostic methods for ORT include isolation and identification through biochemical testing, agglutination-based serotyping, and PCR-based assays targeting the 16S rRNA or *rpoB* genes (Van Empel et al., 1997; Veiga et al., 2019). Although these techniques confirm the

* Corresponding author at: Department of Poultry Diseases, Faculty of Veterinary Medicine, University of Warmia and Mazury, ul. Oczapowskiego 14, Olsztyn 10-719, Poland.
*E-mail addresses:* blanda6@interia.pl (M. Blanda), olimpia.kursa@piwet.pulawy.pl (O. Kursa), joanna.kowalczyk@uwm.edu.pl (J. Kowalczyk), marcin.smialek@uwm.edu.pl (M. Śmiałek).
[1] Contributed equally in leading the work at various stages of the project

https://doi.org/10.1016/j.vetmic.2026.110908
Received 20 November 2025; Received in revised form 5 January 2026; Accepted 27 January 2026
Available online 27 January 2026

presence of ORT, they provide limited insights into its genetic variability, virulence potential, and mechanisms of adaptation. Whole-genome sequencing (WGS) overcomes these limitations by enabling high-resolution genotyping and systematic screening of resistance- and virulence-associated genes (VAGs). WGS data support multilocus sequence typing (MLST), identification of VAGs and resistance determinants, and genome-wide SNP-based phylogenetic inference (Zehr et al., 2014; Alispahic et al., 2021).

Recent advances in WGS have substantially improved the characterization of bacterial pathogens, including those affecting poultry, by enabling standardized, genome-based comparisons across large isolate collections. However, relatively few studies have applied WGS to ORT, and genome-based data remain limited compared with other avian bacterial pathogens (Palmieri et al., 2025; Smith et al., 2020).

In this study, we applied WGS to characterize ORT isolates obtained from turkeys with respiratory and joint infections in Poland between 2018 and 2024. We analysed sequence types, antimicrobial resistance genes, virulence-associated genes, mobile genetic elements, and performed whole-genome core SNP–based phylogenetic analysis to explore the genomic diversity of this pathogen. Using core-genome SNP-based phylogenetic analysis combined with MLST, this study provides a genome-based overview of Polish ORT isolates, contributing to a broader understanding of their epidemiology and antimicrobial resistance in avian hosts.

## 2. Material and methods

For this study, we used samples collected between 2018 and 2024 from 57 turkey flocks located in different regions of Poland. Flocks were sampled only once during the study period. The samples were taken by veterinarians specializing in poultry. Swab samples were taken from birds of both sexes. Birds showed either respiratory signs (including sneezing, swollen sinuses, and serous nasal discharge) or joint lesions. Respiratory samples consisted of tracheal and/or sinus swabs obtained from birds with respiratory signs (n = 41 flocks). In flocks with joint lesions, necropsies were performed on birds that had died naturally or were euthanized for welfare reasons, and joint swabs were collected (n = 16 flocks). Birds displaying typical macroscopic joint lesions, such as joint swelling, were selected for bacteriological examination. Information on sex and age was not consistently available for all birds. Vaccination status was available for most flocks and is provided for descriptive purposes only; approximately 90 % of flocks from which respiratory samples were collected had been vaccinated against ORT, whereas flocks yielding joint-derived samples were unvaccinated. All the samples were sent to the laboratory of the National Veterinary Research Institute under refrigerated conditions and processed immediately upon arrival.

### 2.1. ORT strain isolation and identification

Swabbed samples obtained from the birds were streaked onto tryptone soy agar (TSA) with the addition of sterile defibrinated sheep blood (TSA PS 22–500, Graso Biotech, Starogard Gdański, Poland and sheep blood SL0160–500, BioMaxima S.A., Lublin, Poland) and incubated in an atmosphere enriched with 5 % $CO_2$ at 37 ± 1 °C for 48 ± 3 h. The microbial species were identified using matrix-assisted laser desorption/ionization–time-of-flight mass spectrometry and compared with reference spectra (Biotyper, Bruker, Billerica, MA, USA). Genomic DNA was extracted from isolates identified as ORT using a Maxwell® RSC Cultured Cells DNA kit (Promega, Madison, WI, USA) with a Maxwell® RSC Instrument (Promega) in accordance with the manufacturer's instructions. Identification of ORT was confirmed by PCR targeting the *rpoB* gene using previously described primers (Veiga et al., 2019).

### 2.2. Whole-genome sequencing

One representative isolate per flock was selected for WGS, for which purified DNA was used. DNA extracts were subsequently measured with a NanoDrop™ One UV-Vis spectrophotometer for yield and purity checks (Thermo Scientific, Waltham, MA, USA). DNA libraries were prepared with a KAPA HyperPlus kit (Roche, Basel, Switzerland) according to the manufacturer's instructions. The isolates were sequenced at 2 × 150 bp using the NextSeq platform (Illumina, Inc., San Diego, CA, USA) (Supplementary File 1).

### 2.3. In silico analyses and genome quality control

Initial quality control was carried out with the use of SeqKit (fasta, fatq) version 2.9.0, CheckM version 1.2.3 and QUAST version 5.3.0 (Shen et al., 2016; Gurevich et al., 2013). The reads were trimmed using fastp 0.20.0 (Chen, 2023). Corrected reads were merged by bbmerge (Bushnell et al., 2017) and assembled *de novo* using SPAdes 3.9.0 (Prjibelski et al., 2020). Assemblies were evaluated based on genome size, GC content, completeness, contamination, N50 value, and number of contigs. Only assemblies with parameters consistent with reference ORT genomes and fewer than 300 contigs were retained. Of the 49 sequenced isolates, 47 passed all quality control criteria and were included in a core-genome SNP-based phylogenetic analysis derived from whole-genome sequence data.

### 2.4. Core-genome SNP-based phylogenetic analysis

Core SNPs were identified from the trimmed, paired-end reads against the reference genome GCA_000756505.1_ASM75650v1_genomic.fna (ORT-UMN 88) using Snippy v. 4.6.0 with default parameters (Seemann, 2022). The core SNP alignment was run through Gubbins v. 3.1.0 to remove SNPs found in recombinant regions from the alignment. Non-recombinant SNP positions containing missing data were extracted to produce a SNP-only alignment with snp-sites v. 2.5.1. A maximum-likelihood phylogenetic tree was constructed from this alignment using IQ-TREE with the GTR+G model and branch support assessed using 1000 ultrafast bootstrap replicates and 1000 SH-aLRT replicates. Phylogenetic trees were visualized using iTOL version 7 (Letunic and Bork, 2021).

### 2.5. Detection of antimicrobial resistance genes, virulence-associated genes and mobile genetic elements

Antimicrobial resistance (AMR) determinants were initially screened using ABRicate version 1.0.1 with a minimum identity threshold of 90 % and a minimum gene coverage of 40 %. These thresholds were applied to allow sensitive detection of truncated or partially conserved resistance genes, which may result from genome fragmentation or association with mobile genetic elements (Zhou et al., 2025). In parallel, AMR genes were identified using ResFinder version 4.7.2 with default parameters. Only resistance determinants confirmed by ResFinder were included in the final analysis and interpretation (Florensa et al., 2022).

Virulence-associated genes were identified using ABRicate with the VFDB database and plasmid content was screened using PlasmidFinder version 2.0.1 (Carattoli and Hasman, 2020). The harbouring of resistance genes in relation to MGE presence was tested with the use of Mobile Element Finder (MGEfinder version 1.0.3) provided by the Center for Genomic Epidemiology (Johansson et al., 2021).

### 2.6. Multilocus sequence typing

The WGS sequences were added to the PubMLST database, where their sequence types were determined based on seven housekeeping genes (*adk*, *aroE*, *fumC*, *gdhA*, *mdh*, *pgi*, and *pmi*) (Thieme et al., 2016). Isolates with hitherto unidentified MLST profiles were assigned a new ST

number. Phylogenetic analysis of MLST sequences of Polish and other European ORT isolates included in the PubMLST database was performed using the PHYLOViZ Online program (Ribeiro-Gonçalves et al., 2016). The iTOL version 7 tool was used to generate the phylogenetic tree (Letunic and Bork, 2021). MLST-based analyses were performed independently of the SNP-based phylogenetic reconstruction and were used exclusively for sequence type assignment and comparative typing.

## 3. Results

### 3.1. ORT isolation and identification

In total, 49 ORT isolates were obtained from samples collected from 57 turkey flocks between 2018 and 2024. Of these isolates, 33 originated from flocks with respiratory signs and 16 from flocks with joint lesions. All isolates were identified by MALDI-TOF MS and subsequently confirmed as ORT by PCR targeting the *rpoB* gene. The list of samples is presented in Supplementary File 1.

### 3.2. Whole-genome sequencing and quality control

Whole-genome sequencing was performed for 49 isolates, of which 47 passed all quality control criteria and were included in downstream analyses. Initial quality control of the genome sequences based on the QUAST report showed that the GC contents of the isolates were between 37.12 % and 37.85 %, the numbers of contigs were 33–207, and the total lengths of the complete genome after assembly were 2.1–2.4 Mbp (Supplementary File 1). The sequence data analysed in this study are publicly available in the NCBI database under BioProject PRJNA1307273. Individual accession and BioSample numbers are listed in Supplementary File 1. WGS sequences are also available in the PubMLST database.

### 3.3. Whole-genome SNP-based phylogenetic analysis

Whole-genome core SNP–based phylogenetic analysis was performed for all isolates passing quality control (n = 47). The SNP-based phylogeny resolved the analysed isolates into four major genetic groups based on SNP clustering (Fig. 1). Core-genome SNP analysis revealed a clear phylogenetic structure among the analysed ORT isolates. The maximum-likelihood tree based on non-recombinant core SNPs showed clustering that was largely consistent with MLST sequence types, with ST46 forming a distinct and well-supported clade comprising the majority of isolates. This lineage displayed limited internal diversification, with short branch lengths indicating a high degree of genomic similarity among ST46 isolates.

Isolates belonging to ST3 formed a separate, well-defined cluster that was clearly separated from the ST46 lineage. Additional sequence types,

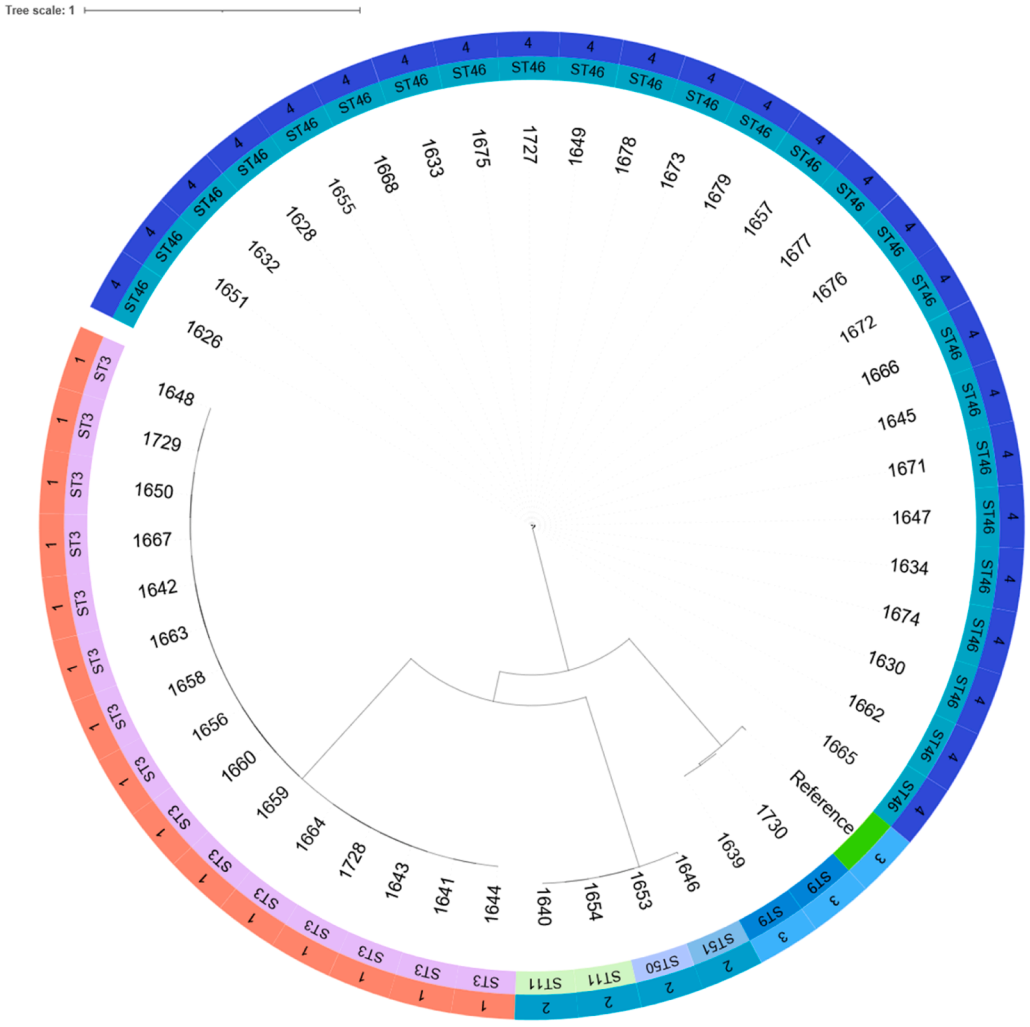


**Fig. 1.** Core-genome SNP–based maximum-likelihood phylogenetic tree of *O. rhinotracheale* isolates inferred from non-recombinant core SNPs using IQ-TREE (GTR+G model). Isolates are labelled by sequence type (ST), and the reference genome ORT-UMN 88 is included. The scale bar indicates substitutions per site. Tree created using iTOL v7.

including ST11, ST50, ST51, and ST9, were positioned outside the dominant ST46 clade and showed greater phylogenetic distances relative to one another, consistent with higher genomic divergence. The reference genome clustered outside the major ST46 group, serving as an external anchor for tree topology (Fig. 1).

### 3.4. Antimicrobial-resistance and virulence-associated genes

Antimicrobial resistance genes reported in this section were identified using ResFinder version 4.7.2 with default parameters. Genomic analysis of the isolates revealed the presence of multiple antimicrobial-resistance determinants. The tetracycline resistance gene *tetQ* (ribosomal protection protein) was highly prevalent, detected in 91.5 % of isolates (90.3 % of those from the respiratory tract and 93.8 % of those from joints). In contrast, the tetracycline-inactivating gene *tetX* (monooxygenase) was identified in only 34.0 % of isolates (48.4 % of those from the respiratory tract and 6.3 % of those from the joints). The macrolide resistance gene *ermF* (erythromycin ribosomal methylase) was found in 95.7 % of isolates, occurring in high numbers in both respiratory (93.6 %) and joint (100 %) samples. The carbapenem resistance gene *blaORR-1* (subclass B1 metallo-β-lactamase) was present in 40.4 % of isolates, with a higher frequency in joint isolates (50 %) than in respiratory ones (35.5 %). Additionally, the macrolide resistance gene *mefA* (efflux protein A) and the aminoglycoside resistance gene *aadS* (6-adenylyltransferase) were identified, which were both present in one isolate (6.3 %) from a joint (Table 1, Fig. 2).

Several VAGs were found, including *ureB* (urease subunit β) and *ureG*, *ureF*, and *ureE* (urease accessory proteins G, F, and E) which activate urease. This enzyme helps colonization and causes damage to the mucous membrane through the toxic effects of ammonia (Abd El-Ghany, 2021; Vandamme et al., 1994). The *tviB* gene encoding UDP-N-acetylglucosamine C-6 dehydrogenase for Vi polysaccharide biosynthesis was identified in 45.1 % of isolates from the respiratory tract and 87.5 % of isolates from joints. This gene is crucial for the formation of the Vi antigen, and thus for bacterial virulence and their ability to evade the host's immune response (Zhang et al., 2022). The *tuf*A gene encoding elongation factor Tu (EF-Tu), a multifunctional protein implicated in bacterial adhesion and virulence, was detected in all isolates (Kaufmann et al., 2025). Similarly, the groEL gene encoding the GroEL chaperonin, which contributes to stress tolerance and survival under adverse conditions, was universally present (Hennequin et al., 2001). All ORT isolates have also a haemolysin family protein, which is a putative virulence determinant (Abd El-Ghany, 2021). Genes encoding core components of the clustered regularly interspaced short palindromic repeats CRISPR – Cas system, including *cas1*, *cas2*, and *cas9*, were identified in the analyzed genomes (Horvath and Barrangou, 2010). All isolates contained the *GldD*, *GldJ*, *GldN*, and *GldH* gliding motility-associated genes, responsible for ABC transporter lipoproteins, as well as *GldK*, *GldL*, *GldG*, *GldM*, and *GldE*, involved in protein secretion (Shrivastava et al., 2013). The isolates contained VAGs, including those encoding toxins and antitoxins from multiple families: the Txe/YoeB addiction module toxin, Phd/YefM and RelE/ParE type II toxin-antitoxin systems, the zeta toxin family, the AbiEi type IV antitoxin domain-containing protein, and the nucleotidyl transferase AbiEii/AbiGii toxin family (Van Melderen, 2010; Mutschler et al., 2011; Dy et al., 2014) Fig. 2. A summary of virulence-associated genes identified in the analysed isolates is provided in or Supplementary File 2.

### 3.5. Multilocus sequence types of ORT

Multilocus sequence typing identified six sequence types among the analysed isolates. Known STs included ST3 (n = 15), ST9 (n = 2), and ST11 (n = 2). The remaining isolates were assigned to three novel sequence types, designated ST46 (n = 26), ST50 (n = 1), and ST51 (n = 1). Most of the isolates from joints were the new ST46 (n = 14), with the remaining ones being ST3 (n = 1) and ST9 (n = 1) (Fig. 3). All isolates fell within four clades. Clade 1 was composed of isolates of ST3 (n = 15). Clade 2 comprised ORT isolates of ST11 (n = 2) and ST50 and ST51 (n = 1 each). Clades 3 and 4 were exclusively ST9 (n = 2) and ST46 (n = 26) isolates, respectively (Figs. 1 and 2). The MLST-based minimum spanning tree showed a structured population of ORT sequence types, with closely related STs forming interconnected clusters (Fig. 4). Colouring by host species and country of origin indicated that several STs were shared among different avian hosts and across multiple European countries, without clear host- or country-specific clustering. Consistently, the MLST-based phylogenetic tree constructed from concatenated allelic profiles placed Polish isolates within multiple clades together with isolates from other European countries (Fig. 5), supporting the presence of widely distributed MLST lineages circulating across diverse hosts and geographic regions.

### 3.6. Sequence type–associated profiles of resistance and virulence-related genes

All ST3 isolates showed 100 % presence of the resistance genes *ermF*, *tetQ*, and *tetX*. All ST46 isolates harboured *ermF* and *tetQ*, and 73 % additionally carried the β-lactam resistance gene *blaORR-1*. Isolates belonging to other sequence types were represented by smaller numbers. ST11 isolates (n = 2) carried only *ermF*. The ST50 isolate contained *tetQ* only, while the ST51 isolate carried *ermF* and *tetX*. For ST9, one respiratory isolate carried *tetQ* only, whereas the joint-derived isolate harboured *ermF* together with *aadS* and *mefA* (Figs. 2 and 6).

Analysis of virulence-associated genes and toxin–antitoxin systems revealed ST-dependent presence patterns. All ST46 isolates carried *tviB*

**Table 1**
Antimicrobial resistance genes detected among *Ornithobacterium rhinotracheale* isolates analysed in this study (n = 47).

| Gene | AMR gene family | Drug class | Antibiotic | % Identity of matching region | Respiratory isolates (n = 31) | Joint isolates (n = 16) |
|---|---|---|---|---|---|---|
| *tet*X | tetracycline-resistant ribosomal protection protein | tetracyclines | minocycline, tetracycline, doxycycline, tigecycline | 100 | 15 (48.4 %) | 1 (6.3 %) |
| *tet*Q | tetracycline-resistant ribosomal protection protein | tetracyclines | minocycline, tetracycline, doxycycline | 100 | 28 (90.3 %) | 15 (93.8 %) |
| *erm*F | erythromycin ribosomal methylase | macrolides streptogramin B | clindamycin, lincomycin, quinupristin, pristinamycin IA, virginiamycin S, erythromycin | 100 | 29 (93.6 %) | 16 (100 %) |
| *bla*ORR-1 | subclass B1 metallo-β-lactamase | β-lactam antibiotics | β-lactam antibiotics | 100 | 11 (35.5 %) | 8 (50 %) |
| *aad*S | aminoglycoside 6-adenylyltransferase | aminoglycosides | streptomycin | 100 | 0 (0 %) | 1 (6.3 %) |
| *mef*A | macrolide efflux protein A | macrolides | erythromycin azithromycin | 99.5 | 0 (0 %) | 1 (6.3 %) |

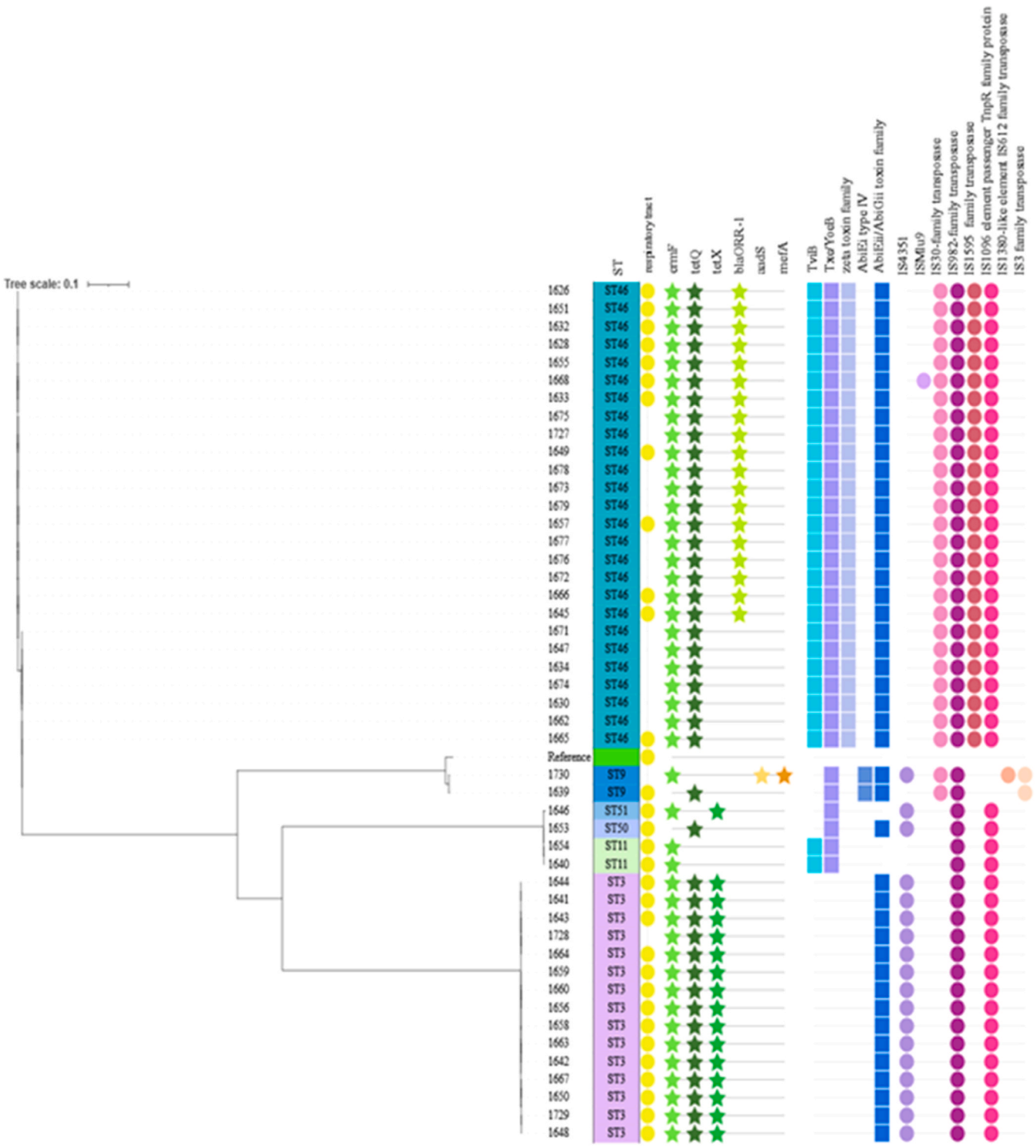


**Fig. 2.** Core-genome SNP–based phylogeny of *Ornithobacterium rhinotracheale* isolates with associated genomic features.Maximum-likelihood phylogenetic tree constructed from core-genome SNPs of *O. rhinotracheale* isolates. The tree is annotated with sequence types (STs) and isolate origin (respiratory or joint). Presence–absence patterns of antimicrobial resistance genes, selected virulence-associated genes, and insertion sequences are shown alongside the phylogeny. Genomic feature profiles are shown for the analyzed isolates only; data for the reference genome are not included in the AMR, VAG, or IS annotations. Only VAGs displaying sequence type–dependent distribution patterns are presented. Tree prepared using iTOL v7.

and genes encoding the Txe/YoeB, Phd/YefM, RelE/ParE, zeta toxin, and AbiEii/AbiGii toxin families, whereas the AbiEi type IV antitoxin was not detected in this ST. ST3 isolates consistently carried Phd/YefM, RelE/ParE, and the AbiEii/AbiGii toxin family, while *tviB*, Txe/YoeB, the zeta toxin family, and AbiEi were absent. ST11 isolates carried *tviB* together with Txe/YoeB, Phd/YefM, and RelE/ParE, but lacked the zeta toxin and AbiE families. The ST50 isolate carried Txe/YoeB, Phd/YefM, RelE/ParE, and AbiEii/AbiGii, whereas *tviB*, the zeta toxin family, and AbiEi were absent. The ST51 isolate carried Txe/YoeB, Phd/YefM, and RelE/ParE only. Both ST9 isolates carried Txe/YoeB, Phd/YefM, RelE/ParE, AbiEi, and AbiEii/AbiGii, while *tviB* and the zeta toxin family were not detected (Fig. 2).

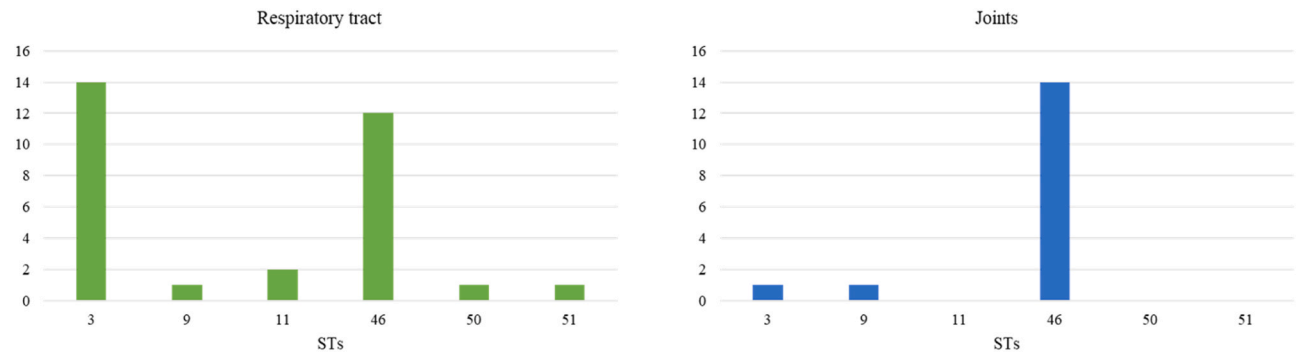


**Fig. 3.** Distribution of *O. rhinotracheale* sequence types by anatomical site of isolation.Number of *O. rhinotracheale* isolates assigned to individual sequence types (STs) among isolates recovered from the respiratory tract and from joints. Bars represent the number of isolates per sequence type for each anatomical site. (a) Isolates recovered from the respiratory tract. (b) Isolates recovered from joints. Y-axis: Number of isolatesX-axis: Sequence type (ST).

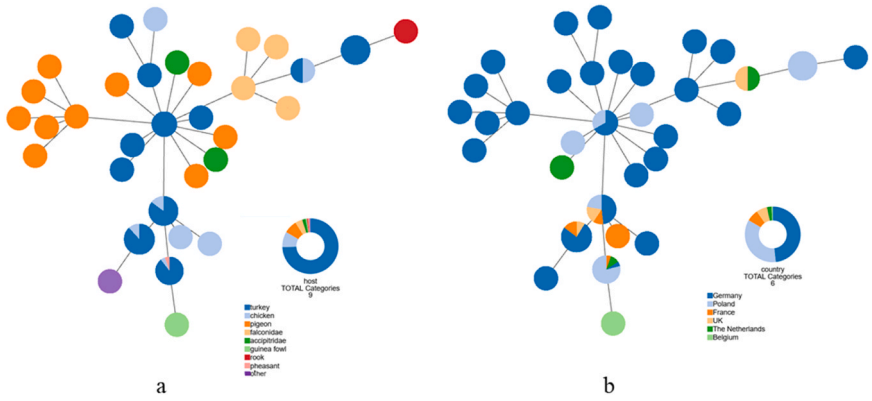


**Fig. 4.** MLST-based minimum spanning tree of *O. rhinotracheale* sequence types. Tree generated using PHYLOViZ Online. Minimum spanning tree constructed based on the seven-locus MLST scheme. Each node represents a sequence type (ST), and edges indicate allelic relatedness between STs. (a) Nodes colored according to host species. (b) Nodes colored according to country of origin. Pie charts summarize the number of host species or countries associated with individual STs.

### *3.7. Mobile genetic elements*

The tested ORT isolates also harboured MGEs like IS4351 (IS30 family). Except for one that was associated with the *tetQ* resistance gene, the MGEs were not associated with any resistance gene. The occurrence of the resistance-gene–associated MGE was not associated with every ST: this one, IS4351, was present in all ST3, ST50, and ST51 isolates and one ST9 isolate from joints, but was absent from ST11 and ST46 isolates. Insertion sequence Mlu9 from the IS481 family was detected in one ST46 isolate from the respiratory tract (Fig. 2). Analysis of sequences deposited in the GenBank database revealed the presence of additional insertion sequences; in addition, several insertion sequence families, including the family transposase IS982, IS30, IS1595, IS3, and the IS1380-like element IS612 family transposase, were identified, with their distribution showing associations with specific sequence types (Fig. 2; Supplementary File 2).

### *3.8. Plasmid identification*

No plasmid was identified in any of the ORT isolates using the described tools.

## 4. Discussion

Knowledge of the genomic diversity of clinical respiratory and joint ORT isolates occurring in turkey production remains limited. Therefore, we undertook this study to provide genomic and epidemiological insight into ORT infections by sequencing isolates from clinical cases of respiratory and joint infections. Through whole-genome sequencing, we examined STs, antimicrobial resistance, VAGs, and genome-wide lineage relationships inferred from core-genome SNP-based phylogenetic analysis, contributing to an improved understanding of the genomic diversity of *O. rhinotracheale* isolates circulating in turkey populations.

The multilocus sequence typing and comparative analysis of genome-wide SNP variation and selected genomic features revealed considerable genetic diversity among Polish isolates. Of the six different STs identified, three were newly described in this study, demonstrating ongoing diversification of ORT in turkey populations. The predominance of ST3 and ST46 – particularly in isolates from birds with respiratory and joint lesions – suggests that these sequence types may possess enhanced virulence or host adaptation potential. This pattern contrasts with data from Western Europe and the USA, where ST1, ST9, and ST11 dominate in turkey isolates (Fig. 4) (Smith et al., 2020). The identification of novel sequence types highlights regional diversity and underscores the importance of continued genomic surveillance across different geographic areas.

The phylogenetic clustering of isolates into four major groups reflects genome-wide lineage differentiation inferred from core-genome SNP-based phylogenetic analysis. ST3, ST9, and ST46 formed distinct clusters, whereas ST11, ST50, and ST51 clustered more closely in the SNP-based phylogenetic analysis, indicating differences in genome-wide relatedness among these sequence types. (Fig. 1). Such genomic differentiation could underlie variations in tissue tropism, virulence potential, or antimicrobial susceptibility, warranting further functional investigation.

Our analysis of antimicrobial resistance genes revealed widespread presence of genes conferring resistance to tetracyclines, macrolides, and β-lactams, consistent with earlier reports (Chrzastek et al., 2025). The

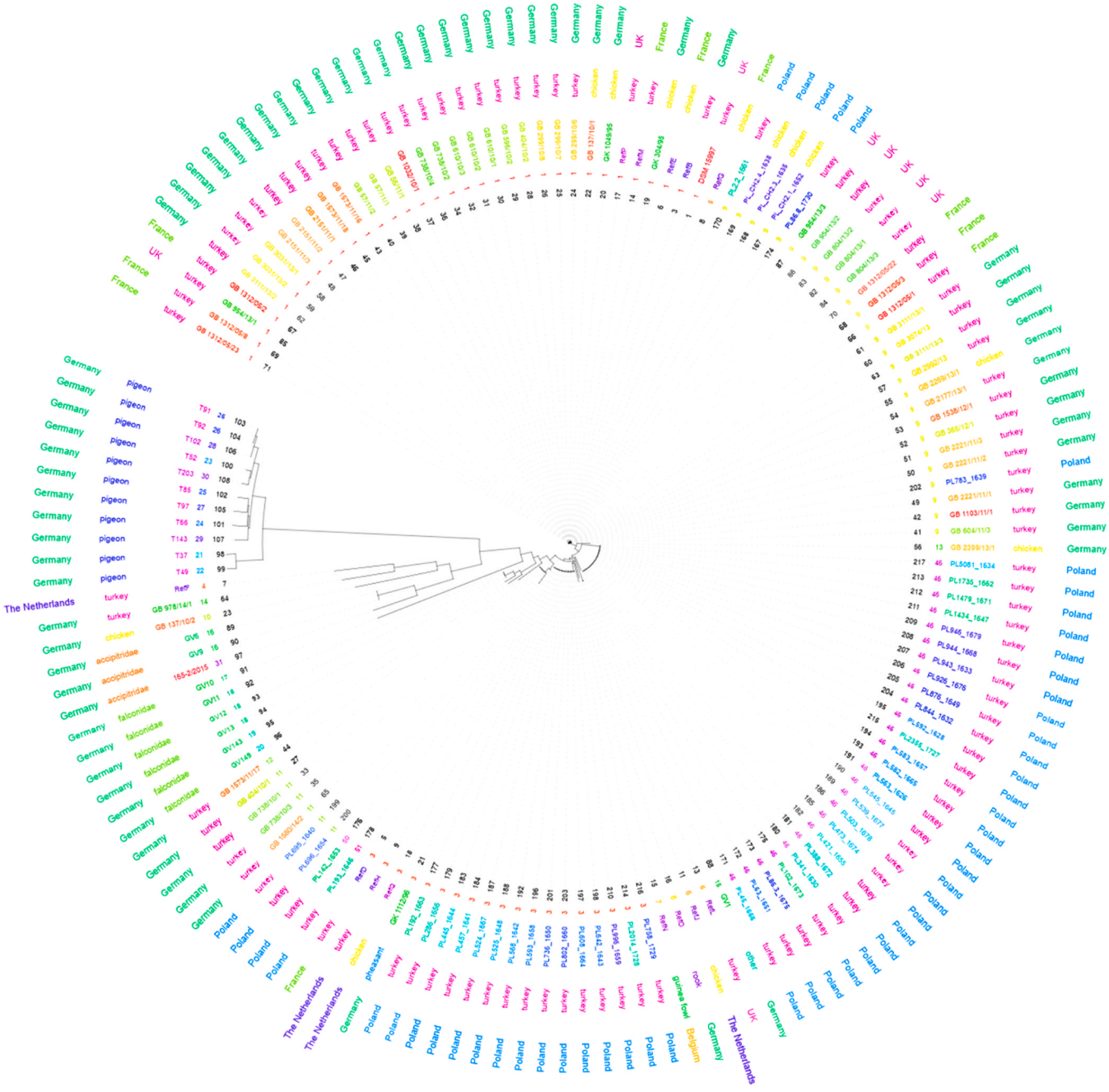

**Fig. 5.** MLST-based phylogenetic tree of *O. rhinotracheale* isolates in a global context.Phylogenetic tree constructed based on concatenated sequences of the seven-locus MLST scheme. Polish isolates analyzed in this study are shown together with publicly available *O. rhinotracheale* MLST profiles retrieved from the PubMLST database. Tip labels are colored according to host species and country of origin, as indicated. The dashed red line highlights the clustering of Polish isolates within the global MLST diversity. Tree created using iTOL v7.

nearly universal detection of *ermF* and *tetQ* across isolates highlights the persistence of multidrug-resistance determinants within ORT populations (Fig. 2). However, differences in resistance gene composition between respiratory and joint isolates suggest selective pressures that may vary with the anatomical site of infection. For example, *blaORR-1* was more prevalent in joint isolates. Interestingly, the *tetQ* and *tetX* genes were not detected in one joint isolate, which carried only the *ermF* gene. The presence of *ermF* in joint isolates was 100 % and in respiratory isolates 93.5 %, while that of *tetQ* was 93.7 % and 90.3 %, respectively. However, when *tetX* was detected, it was found mainly in respiratory isolates and in only one joint isolate. This uneven distribution may suggest a role of *tetX* in environments characterized by higher antimicrobial pressure or metabolic activity, such as the respiratory tract, where exposure to aerosolized antimicrobials and oxygen tension may facilitate horizontal gene exchange. The consistent presence of *ermF* and *tetQ* across nearly all isolates indicates that these determinants represent stably maintained resistance markers within ORT populations.

We also conducted the first analysis of resistance genes by sequence type, and the results did not differ depending on the anatomical site of isolation. In each ST3 isolate, 100 % presence of the *ermF*, *tetQ*, and *tetX* resistance genes was found, reflecting a multidrug-resistant genotype that may contribute to the predominance of this lineage in clinical outbreaks. In ST46 isolates, 100 % harboured *ermF* and *tetQ*, and 73 % also contained the β-lactam resistance gene *blaORR-1*, indicating that this emerging sequence type is characterized by the presence of additional resistance determinants compared with other sequence types.

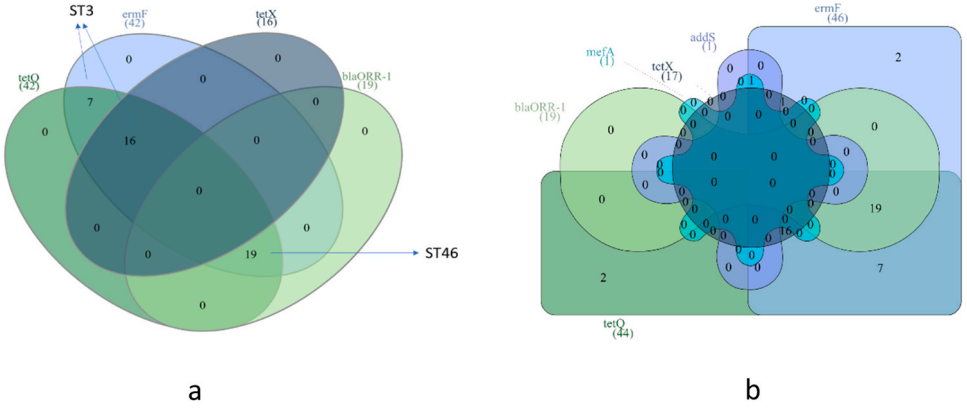


**Fig. 6.** Co-occurrence of antimicrobial resistance genes among *O. rhinotracheale* isolates.Venn diagrams illustrating the presence and co-occurrence of selected antimicrobial resistance genes detected in whole-genome sequences. (a) Distribution of resistance genes among isolates assigned to ST3 and ST46. (b) Distribution of resistance genes across all sequence types. Numbers indicate the number of isolates carrying individual genes or gene combinations.

Isolates of ST11 harboured only the *ermF* gene, the ST50 isolate contained only *tetQ*, while ST51 carried both *ermF* and *tetX*. The case of ST9 is particularly noteworthy: one isolate from the respiratory tract contained only *tetQ*, while the ST9 isolate from the joint carried *ermF* together with *aadS* and *mefA* – the latter two found exclusively in this isolate. The presence of the macrolide efflux pump encoder *mefA* together with *ermF* suggests potential redundancy in macrolide resistance mechanisms, which could enhance survival under therapeutic exposure. Such lineage-specific combinations of resistance determinants underline the genomic flexibility and adaptive potential of ORT, which enable it to persist under diverse environmental and pharmacological pressures.

The detection of virulence-associated genes and putative toxins, including haemolysin family proteins, suggests that ORT possesses multiple mechanisms that contribute to host colonization and pathogenicity. Haemolysins, known for their cytotoxic and membrane-disrupting activity, also play key roles in host–pathogen interactions, facilitating tissue invasion and immune evasion (Abd El-Ghany, 2021; Li et al., 2018). The consistent presence of these factors across isolates indicates that they may represent core virulence components of ORT, potentially modulated by other genomic features or environmental cues.

The identification of the IS4351 and ISMlu9 MGEs provides novel evidence of the genomic flexibility and adaptive potential of ORT. These elements are known to mediate genome rearrangements, horizontal gene transfer, and regulatory changes that can drive the emergence of new phenotypes, including antimicrobial resistance (Rasmussen et al., 1987; Podglajen et al., 2001). Their detection in specific sequence types – particularly ST3, ST50, and ST51 – indicating lineage-specific differences in the distribution of mobile genetic elements among the analysed isolates. The finding of ISMlu9 in an ST46 isolate further emphasizes the potential of these mobile elements to act as genomic drivers of diversification. Our findings add to earlier reports describing insertion sequences and other mobile genetic elements in ORT. Recent genomic studies have documented IS elements (including IS4351 and IS1380) associated with resistance determinants in ORT isolates, demonstrating that MGEs have previously been observed in this species (Palmieri et al., 2025; Smith et al., 2020; Hashish et al., 2023). The present study extends these observations by documenting the distribution of MGEs across Polish sequence types and by reporting ISMlu9 (IS481 family) in one ST46 isolate, which appears to be novel for ORT. In addition, several insertion sequence families were identified, including the family transposase IS982, IS30, IS1595, IS3, and the IS1380-like element IS612 family transposase, with their occurrence varying across sequence types (Supplementary File 2).

The genome-based analyses presented here expand current knowledge of the genetic diversity and population structure of ORT. Systematic deposition of ORT genomes in public databases is crucial to the effectiveness of ongoing surveillance and global comparative analyses, which may ultimately inform vaccine development and disease control strategies.

In conclusion, this study provides a genomic overview of *O. rhinotracheale* isolates recovered from respiratory and joint lesions in turkeys in Poland. The identification of novel sequence types, lineage-associated resistance profiles, and mobile genetic elements underscores the genetic diversity of ORT populations. These findings enhance current knowledge of ORT epidemiology and provide a foundation for future comparative genomic studies addressing the evolution and control of this pathogen.

## CRediT authorship contribution statement

**Joanna Kowalczyk:** Writing – review & editing, Investigation. **Olimpia Kursa:** Writing – original draft, Visualization, Supervision, Methodology, Investigation, Funding acquisition, Formal analysis, Data curation, Conceptualization. **Smialek Marcin:** Writing – review & editing, Supervision, Methodology, Investigation, Data curation, Conceptualization. **Marek Blanda:** Writing – original draft, Investigation, Conceptualization.

## Funding

The study was funded from subsidy provided by the Ministry of Science and Higher Education under the grant no. S/486 performed in 2022–2025 at the National Veterinary Research Institute, Pulawy, Poland.

## Declaration of Competing Interest

The authors declare that they have no known competing financial interests or personal relationships that could have appeared to influence the work reported in this paper.

## Acknowledgements

We thank Agata Sieczkowska and Sylwia Kazak for their excellent technical assistance. We are also grateful to our colleagues from the Department of Research Support for performing whole-genome sequencing.

## Appendix A. Supporting information

Supplementary data associated with this article can be found in the

online version at doi:10.1016/j.vetmic.2026.110908.

## References


Abd El-Ghany, W.A., 2021. An updated comprehensive review on ornithobacteriosis: a worldwide emerging avian respiratory disease. Open Vet. J. 11, 555–568. https://doi.org/10.5455/OVJ.2021.v11.i4.5.

Vandamme, P., Segers, P., Vancanneyt, M., Van Hove, K., Mutters, R., Hommez, J., Dewhirst, F., Paster, B., Kersters, K., Falsen, E., Devriese, L.A., Bisgaard, M., Hinz, K. H., Mannheim, W., 1994. Ornithobacterium rhinotracheale gen. nov., sp. nov., isolated from the avian respiratory tract. Int J. Syst. Bacteriol. 44, 24–37. https://doi.org/10.1099/00207713-44-1-24.

Devriese, L.A., Hommez, J., Vandamme, P., Kersters, K., Haesebrouck, F., 1995. In vitro antibiotic sensitivity of Ornithobacterium rhinotracheale strains from poultry and wild birds. Vet. Rec. 137, 435–436. https://doi.org/10.1136/vr.137.17.435.

Van Empel, P., Van Den Bosch, H., Loeffen, P., Storm, P., 1997. Identification and serotyping of Ornithobacterium rhinotracheale. J. Clin. Microbiol. 35, 418–421. https://doi.org/10.1128/jcm.35.2.418-421.1997.

Veiga, I.M.B., Lüschow, D., Gutzer, S., Hafez, H.M., Mühldorfer, K., 2019. Phylogenetic relationship of Ornithobacterium rhinotracheale isolated from poultry and diverse avian hosts based on 16S rRNA and rpoB gene analyses. BMC Microbiol. 19, 31. https://doi.org/10.1186/s12866-019-1395-9.

Zehr, E.S., Bayles, D.O., Boatwright, W.D., Tabatabai, L.B., Register, K.B., 2014. Complete genome sequence of Ornithobacterium rhinotracheale strain ORT-UMN 88. Stand Genom. Sci. 9. https://doi.org/10.1186/1944-3277-9-16.

Alispahic, M., Endler, L., Hess, M., Hess, C., 2021. Ornithobacterium rhinotracheale: Maldi-tof ms and whole genome sequencing confirm that serotypes k, l and m deviate from well-known reference strains and numerous field isolates. Microorganisms 9. https://doi.org/10.3390/microorganisms9051006.

Palmieri, N., Hess, C., Pollák, B., Magyar, T., Pinter, K., Doman, M., Bilic, I., Hess, M., 2025. Genomic analysis reveals two dominant strains of Ornithobacterium rhinotracheale in Austria and Hungary with distinct multidrug resistance profiles. Appl. Environ. Microbiol. 91. https://doi.org/10.1128/aem.00569-25.

Smith, E.A., Miller, E.A., Weber, B.P., Aguayo, J.M., Figueroa, C.F., Huisinga, J., Nezworski, J., Kromm, M., Wileman, B., Johnson, T.J., 2020. Genomic landscape of Ornithobacterium rhinotracheale in commercial Turkey Production in the United States. Appl. Environ. Microbiol. 86. https://doi.org/10.1128/AEM.02874-19.

Shen, W., Le, S., Li, Y., Hu, F., 2016. SeqKit: A cross-platform and ultrafast toolkit for FASTA/Q file manipulation. PLoS One 11. https://doi.org/10.1371/journal.pone.0163962.

Gurevich, A., Saveliev, V., Vyahhi, N., Tesler, G., 2013. QUAST: Quality assessment tool for genome assemblies. Bioinformatics 29. https://doi.org/10.1093/bioinformatics/btt086.

Chen, S., 2023. Ultrafast one-pass FASTQ data preprocessing, quality control, and deduplication using fastp. iMeta 2. https://doi.org/10.1002/imt2.107.

Bushnell, B., Rood, J., Singer, E., 2017. BBMerge – accurate paired shotgun read merging via overlap. PLoS One 12. https://doi.org/10.1371/journal.pone.0185056.

Prjibelski, A., Antipov, D., Meleshko, D., Lapidus, A., Korobeynikov, A., 2020. Using SPAdes De Novo assembler. Curr. Protoc. Bioinforma. 70. https://doi.org/10.1002/cpbi.102.

Seemann, T., Snippy: Fast Bacterial Variant Calling from NGS Reads, 2022. https://github.com/tseemann/snippy.

Letunic, I., Bork, P., 2021. Interactive tree of life (iTOL) v5: An online tool for phylogenetic tree display and annotation. Nucleic Acids Res. 49. https://doi.org/10.1093/nar/gkab301.

Zhou, S., Liu, B., Zheng, D., Chen, L., Yang, J., 2025. VFDB 2025: an integrated resource for exploring anti-virulence compounds. Nucleic Acids Res. 53, D871–D877. https://doi.org/10.1093/nar/gkae968.

Florensa, A.F., Kaas, R.S., Clausen, P.T.L.C., Aytan-Aktug, D., Aarestrup, F.M., 2022. ResFinder – an open online resource for identification of antimicrobial resistance genes in next-generation sequencing data and prediction of phenotypes from genotypes. Micro Genom. 8. https://doi.org/10.1099/mgen.0.000748.

Carattoli, A., Hasman, H., 2020. PlasmidFinder and In Silico pMLST: Identification and Typing of Plasmid Replicons in Whole-Genome Sequencing (WGS). In: de la Cruz, F. (Ed.), Horizontal Gene Transfer. Methods in Molecular Biology, 2075. Humana, New York, NY. https://doi.org/10.1007/978-1-4939-9877-7_20.

Johansson, M.H.K., Bortolaia, V., Tansirichaiya, S., Aarestrup, F.M., Roberts, A.P., Petersen, T.N., 2021. Detection of mobile genetic elements associated with antibiotic resistance in Salmonella enterica using a newly developed web tool: MobileElementFinder. J. Antimicrob. Chemother. 76. https://doi.org/10.1093/JAC/DKAA390.

Thieme, S., Mühldorfer, K., Lüschow, D., Hafez, H.M., 2016. Molecular characterization of the recently emerged poultry pathogen ornithobacterium rhinotracheale by multilocus sequence typing. PLoS One 11, 1–12. https://doi.org/10.1371/journal.pone.0148158.

Ribeiro-Gonçalves, B., Francisco, A.P., Vaz, C., Ramirez, M., Carriço, J.A., 2016. PHYLOViZ Online: web-based tool for visualization, phylogenetic inference, analysis and sharing of minimum spanning trees. Nucleic Acids Res. 44. https://doi.org/10.1093/nar/gkw359.

Zhang, L.F., Lepenies, B., Nakamae, S., Young, B., Santos, R., Raffatellu, M., Cobb, B., Hiyoshi, H., Baumler, A., 2022. The Vi capsular polysaccharide of salmonella typhi promotes macrophage phagocytosis by binding the human C-Type Lectin DC-SIGN. mBio. https://doi.org/10.1128/mbio.02733-22.

Kaufmann, H., Salvador, C., Salazar, V.W., Cruz, N., Dias, G.M., Tschoeke, D., Campos, L., Sawabe, T., Miyazaki, M., Maruyama, F., 2025. Genomic repertoire of twenty-two novel vibrionaceae species isolated from marine sediments. Micro. Ecol. 88. https://doi.org/10.1007/s00248-025-02533-0.

Hennequin, C., Porcheray, F., Waligora-Dupriet, A.J., Collignon, A., Barc, M., Bourlioux, P., Karjalainen, T., 2001. GroEL (Hsp60) of Clostridium difficile is involved in cell adherence. Microbiology 147. https://doi.org/10.1099/00221287-147-1-87.

Horvath, P., Barrangou, R., 2010. CRISPR/Cas, the immune system of Bacteria and Archaea. Science 327, 1979. https://doi.org/10.1126/science.1179555.

Shrivastava, A., Johnston, J.J., Van Baaren, J.M., McBride, M.J., 2013. Flavobacterium johnsoniae GldK, GldL, GldM, and SprA are required for secretion of the cell surface gliding motility adhesins sprb and remA. J. Bacteriol. 195. https://doi.org/10.1128/JB.00333-13.

Van Melderen, L., 2010. Toxin-antitoxin systems: Why so many, what for? Curr. Opin. Microbiol. 13 (6). https://doi.org/10.1016/j.mib.2010.10.006.

Mutschler, H., Gebhardt, M., Shoeman, R.L., Meinhart, A., 2011. A novel mechanism of programmed cell death in bacteria by toxin-antitoxin systems corrupts peptidoglycan synthesis. PLoS Biol. 9. https://doi.org/10.1371/journal.pbio.1001033.

Dy, R.L., Przybilski, R., Semeijn, K., Salmon, G., Fineran, P., 2014. A widespread bacteriophage abortive infection system functions through a Type IV toxin-antitoxin mechanism. Nucleic Acids Res. 42. https://doi.org/10.1093/nar/gkt1419.

Chrzastek, K., Seal, B.S., Kulkarni, A., Kapczynski, D.R., 2025. Whole-Genome shotgun sequencing from chicken clinical tracheal samples for bacterial and novel bacteriophage identification. Vet. Sci. 12. https://doi.org/10.3390/vetsci12020162.

Li, Y., Bai, C., Yang, L., Fu, J., Yan, M., Chen, D., Zhang, L., 2018. High flux isothermal assays on pathogenic, virulent and toxic genetics from various pathogens. Micro Pathog. 116. https://doi.org/10.1016/j.micpath.2018.01.006.

Rasmussen, J.L., Odelson, D.A., Macrina, F.L., 1987. Complete nucleotide sequence of insertion element IS4351 from Bacteroides fragilis. J. Bacteriol. 169. https://doi.org/10.1128/jb.169.8.3573-3580.1987.

Podglajen, I., Breuil, J., Rohaut, A., Monsempes, C., Collatz, E., 2001. Multiple mobile promoter regions for the rare carbapenem resistance gene of Bacteroides fragilis. J. Bacteriol. 183. https://doi.org/10.1128/JB.183.11.3531-3535.2001.

Hashish, A., Johnson, T.J., Smith, E., Chundru, D., Williams, M., Macedo, N., Sato, Y., Ghanem, M., El-Gazzar, M., 2023. Complete genome sequences of three ornithobacterium rhinotracheale strains from avian sources, using hybrid nanopore-illumina assembly. Microbiol. Resour. Announc. 12. https://doi.org/10.1128/mra.01059-22.